analogous modes of the respective rings of the symmetrical sandwiches. This indicates that the extent of pure vibrational coupling between the macrocycles is negligible in all of the complexes. This does not imply, however, that the electronic interactions between the rings are small.

The high-frequency regions of the B-state excitation RR spectra of $Ce(OEP)(TPP)^+$ are shown in the top traces of Figures 2 and 3. Comparison of these spectra with those of the neutral complex reveals that the frequencies of certain skeletal modes of both the OEP and TPP rings are shifted upon oxidation. (It should be noted that the band observed at 1347 cm^{-1} in the spectrum of the cation corresponds to ν_{29} and is not due to ν_4 of residual unoxidized material.) The frequencies of several of these modes are compared with those of the neutral complex in Table I. In general, the oxidation-induced frequency shifts are large for skeletal vibrations of the OEP macrocycle and small for those of the TPP ring. In addition, the shifts observed for the OEP and TPP modes of the asymmetrical complex are larger and smaller, respectively, than those observed for the analogous modes of the OEP and TPP rings of the symmetrical sandwiches.[9] The oxidation-induced frequency shifts observed for all three sandwich complexes are compared in Table I. The shifts observed for $Ce(OEP)_2$ and $Ce(TPP)_2$ are labeled $\Delta\nu_{SYM}$(OEP) and $\Delta\nu_{SYM}$(TPP), respectively, while those observed for Ce(OEP)(TPP) are labeled $\Delta\nu_{ASYM}$(OEP) and $\Delta\nu_{ASYM}$(TPP).

Discussion

The observation that the oxidation-induced frequency shifts of the OEP and TPP skeletal modes in the asymmetrical sandwich are larger and smaller, respectively, than those of these vibrations in the symmetrical complexes is consistent with the notion that the electron is removed primarily from a dimer molecular orbital comprised predominantly of an OEP monomer orbital.[6g,h] The positive shifts observed for the ν_2 and ν_{11} modes of the OEP macrocycle are further consistent with this dimer redox orbital being derived from an a_{1u}-like OEP monomer orbital[15,16] as is the case for the symmetrical OEP sandwich complexes.[9a,b] On the other hand, the frequency shifts observed for the ν_2 and ν_{11} modes of the TPP ring in the asymmetrical sandwich, although relatively small, are opposite in direction from those observed for these modes in the symmetrical TPP sandwich.[9c] These shifts are also opposite to those typically observed for a_{2u} porphyrin cations such as $CuTPP^+$ [16] or $Ce(TPP)_2^+$.[9c] The positive shifts observed for ν_2 and ν_{11} modes of TPP upon oxidation of Ce(OEP)(TPP) are in the direction expected for an a_{1u}-like cation.[15,16] This supports the suggestion that strong $\pi\pi$ interactions result in redox orbital reversal for the TPP ring in Ce(OEP)(TPP) relative to $Ce(TPP)_2$ (vide supra).

There is no direct way to relate the magnitude of the oxidation-induced frequency shifts of the skeletal modes of the two porphyrins in Ce(OEP)(TPP) to the relative magnitudes of the coefficients of the redox orbital in the dimer. If the magnitudes of shifts are assumed to be directly proportional to the hole density, it might be estimated that the a_{1u} orbital of OEP contributes ~80% to the dimer orbital. This value was obtained by averaging $|\Delta\nu_{ASYM}/\Delta_{SYM}|$ for the RR bands of OEP or TPP given in Table I. Inherent in this analysis is the assumption that the oxidation-induced shifts of the RR bands of the symmetrical dimers are half as large as those of the analogous bands of monomeric systems. This is true for some bands but not others.[9a,c] Another qualitative estimate of the orbital coefficients can be obtained by determining the eigenvectors of a two by two matrix in which the redox energies of the a_{1u} orbitals of the metallo-OEP and metallo-TPP monomers lie on the diagonal and the off-diagonal elements are adjusted to yield the 200-mV cathodic shift observed for Ce(OEP)(TPP) versus metallo-OEP monomers. Unfortunately, the energy of the a_{1u} orbitals of monomeric metallo-TPP complexes cannot be estimated from redox potentials because all of these complexes are a_{2u}-like cations.[16,17] If the a_{1u} orbital of TPP is placed 2000-3000 cm^{-1} below the a_{2u} orbital, [18] then diagonalization of the two by two matrix yields a dimer redox orbital that is 70-75% OEP-like in character. This estimate is reasonably close to that determined from the RR data considering the crude level of approximation.

The observation that strong $\pi\pi$ interactions perturb the redox orbital ordering in Ce(OEP)(TPP) suggests that the detailed character of the dimer redox orbitals in asymmetrical sandwich complexes can be manipulated with judicious choice of porphyrin ring substituent groups. For example, the oxidation potentials of monomeric metallo-tetrapentylporphyrins (TPnP) are considerably closer to those of metallo-OEP complexes than are those of metallo-TPP systems.[19] This suggests that an asymmetrical sandwich complex such as Ce(OEP)(TPnP) would have a dimer redox orbital in which the two rings contribute much more equally. Finally, the perturbation of the ground state properties of the asymmetrical sandwiches by strong $\pi\pi$ interactions suggests that the properties of the asymmetrical SP dimer in the genetically modified photosynthetic reaction centers[10] may also be subject to such perturbations. The importance of such effects will depend on the magnitude of $\pi\pi$ interactions between the molecules in the SP. This has yet to be determined.

Acknowledgment. We thank Drs. D. Holten and O. Bilsel for providing the Ce(OEP)(TPP) complex and for many insights regarding its electronic properties. This work was supported by Grant GM-36243 (D.F.B.) from the National Institute of General Medical Sciences.

(15) Oertling, W. A.; Salehi, A.; Chung, Y. C.; Leroi, G. E.; Chang, C. K.; Babcock, G. T. *J. Phys. Chem.* **1987**, *91*, 5887.
(16) Czernuszewicz, R. S.; Macor, K. A.; Li, X.-Y.; Kincaid, J. R.; Spiro, T. G. *J. Am. Chem. Soc.* **1989**, *111*, 3860.
(17) Fajer, J.; Davis, M. S. In *The Porphyrins*; Dolphin, D., Ed.; Academic Press: New York, 1978; Vol. IV, pp 197-156.
(18) Gouterman, M. In *The Porphyrins*; Dolphin, D., Ed.; Academic Press: New York, 1978, Vol. III, pp 1-165.
(19) Atamian, M.; Wagner, R. W.; Lindsey, J. S.; Bocian, D. F. *Inorg. Chem.* **1988**, *27*, 1510.

Contribution from the Department of Chemistry, Washington State University, Pullman, Washington 99164-4630

Theoretical Predictions and New Structures of Stacking Patterns for $Cu_nX_{2n}L_2$ Oligomers

Roger D. Willett,* Marcus R. Bond, and George Pon

Received May 22, 1990

Psuedo-planar oligomers of the type $Cu_nX_{2n}L_2$ ($X = Cl^-, Br^-$; $L = Cl^-, Br^-$, or a neutral ligand) aggregate in the solid state thru the formation of long semicoordinate Cu···X bonds between oligomers. A variety of stacking patterns (polymorphs) are observed.[1-4] We have developed a notation to classify these patterns,[5,6] as well as a simple pictorial scheme to illustrate the stacking arrangements.[7] This classification scheme, while useful

(1) Colombo, A.; Menabue, L.; Motori, A.; Pellacani, G. C.; Porzio, W.; Sandrolini, F.; Willett, R. D. *Inorg. Chem.* **1985**, *24*, 2900.
(2) Grigereit, T.; Ramakrishna, B. L.; Place, H.; Willett, R. D.; Pellacani, G. C.; Manfredini, T.; Menabue, L.; Bonamartini-Corradi, A.; Battaglia, L. P. *Inorg. Chem.* **1987**, *26*, 2235.
(3) Manfredini, T.; Pellacani, G. C.; Bonamartini-Corradi, A.; Battaglia, L. P.; Guarini, G. G. T.; Giusti, J. G.; Pon, G.; Willett, R. D.; West, D. X. *Inorg. Chem.* **1990**, *29*, 2221.
(4) Fletcher, R.; Livermore, J.; Hansen, J. J.; Willett, R. D. *Inorg. Chem.* **1983**, *22*, 330.
(5) Geiser, U.; Willett, R. D.; Lindbeck, M.; Emerson, K. *J. Am. Chem. Soc.* **1986**, *108*, 1173.
(6) Bond, M. R.; Willett, R. D. *Inorg. Chem.* **1989**, *28*, 3267.

0020-1669/90/1329-4160$02.50/0

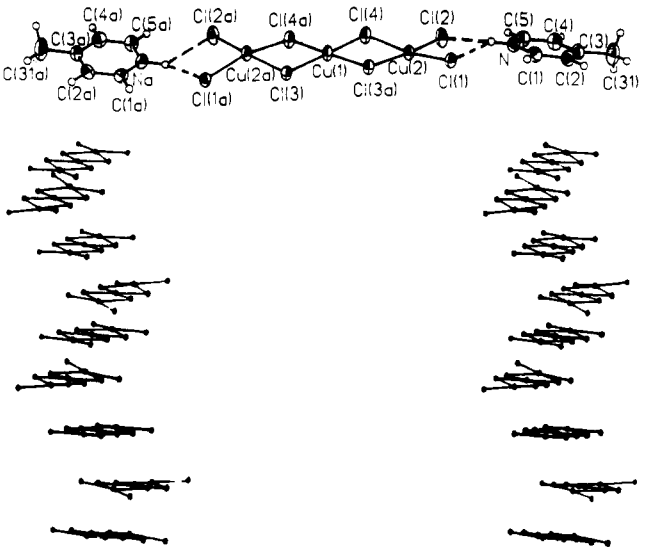

Figure 1. Top: (a) ORTEP drawing of the formula unit for (4-methylpyridinium)$_2$Cu$_3$Cl$_8$. Bottom: (b) Sterographic pair illustration of the stacking of $Cu_3Br_8^{2-}$ anions in (4-methylpyridinium)$_2$Cu$_3$Br$_8$. Semicoordinate bonds are omitted for clarity.

for systematization, is limited in its predictive capability. In this note, we report the structures of compounds containing two new stacking patterns, as well as preliminary results of a phenomenological theory to predict the possible stable phases for a subset of the observed types of stacking patterns.

Recent structure determinations in this laboratory have included the (4-methylpyridinium)$_2$Cu$_3$X$_8$ and Cu$_2$X$_4$(4,4′-dimethyl-2,2′-bipyridine) systems. The 4-methylpyridinium salts contain nearly planar, bridged trimeric $Cu_3X_8^{2-}$ anions.[8,9] Each pyridinium cation forms a bifurcated hydrogen bond to a terminal pair of halide ions. This yields an extended coplanar cation–anion–cation unit (Figure 1a). These units are very similar for X = Cl and X = Br. The $Cu_3Cl_8^{2-}$ oligomers adopt the pattern in I, while planar $Cu_3Br_8^{2-}$ oligomers assume a new stacking pattern, II, as illustrated in Figure 1b. The bipyridine complexes[10,11] contain

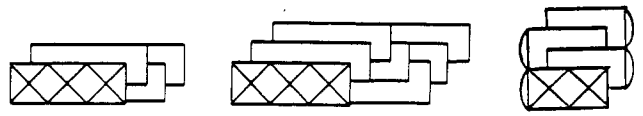

I II III

dimeric units in which one end of each oligomer is capped by the bidentate ligand (Figure 2). The pattern adopted, III, has not previously been observed for $n > 1$. A 180° rotation is associated with each displacement, which minimizes steric repulsions between the bidentate ligands. Full structural data for both pairs of compounds will be published at a later data.[12,13]

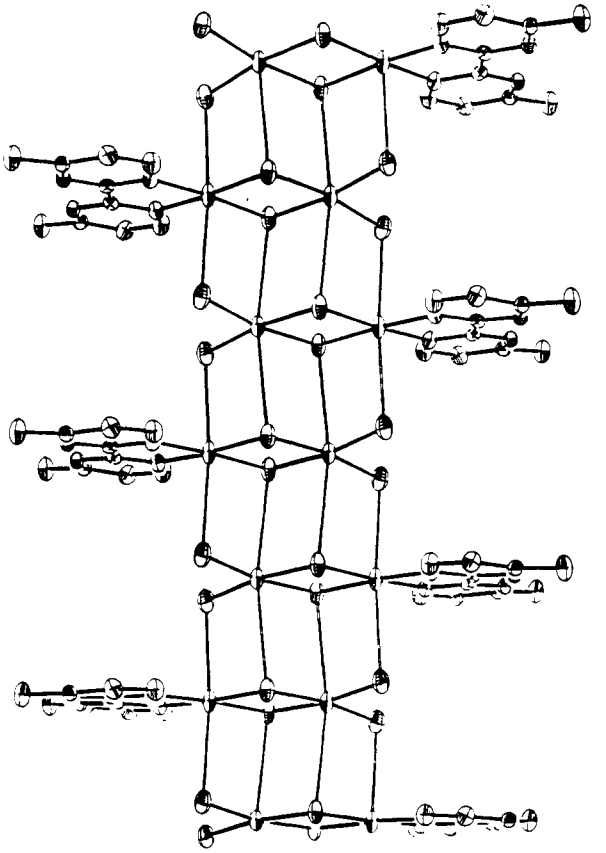

Figure 2. Illustration of the stacking of $Cu_2Cl_4L^2$ oligomers in Cu$_2$Cl$_4$-(4,4′-dimethyl-2,2′-bipyridine).

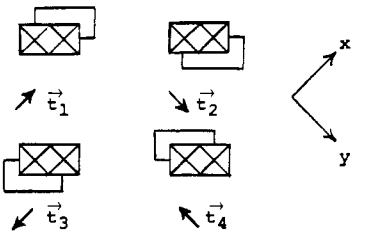

Figure 3. Translations for the subset of stacking patterns of $Cu_nX_{2n}L_2$ oligomers to be considered.

The impetus for seeking a spin-Hamiltonian approach to predict stable stacking patterns is based on the successful application of the next-nearest-neighbor Ising model to a variety of polytyptic[14,15] and magnetic systems.[16,17] For the latter, this yields the usual ferromagnetic and antiferromagnetic states as well as a ↑↑↓↓ sequence arising from competition between the nearest-neighbor and next-nearest-neighbor interactions.[18-20]

The spin-Hamiltonian to describe the polytypism in the $Cu_nX_{2n}L_2$ oligomer systems will necessarily be more complex. If the polytypes are limited to the cases based on the four translations, $\vec{t}_i$, shown in Figure 3 for $n = 2$, a four-state system is defined. An xy model with cubic anisotropy, in which the spins are restricted to orientations parallel to the projection of the $\vec{t}_i$ vectors onto the XY plane, is suggested. Because of the XY nature of the model,

(7) Geiser, U.; Willett, R. D. *Chem. Croat. Acta* **1984**, *57*, 751.
(8) Structural parameters for (4-methylpyridinium)$_2$Cu$_3$Cl$_8$: monoclinic, space group $C2/c$, a = 24.578 (5) Å, b = 12.278 (2) Å, c = 7.106 (1) Å, β = 95.01 (1)°, Z = 4, ρ = 2.06 g/cm^3, μ = 39.8 cm^{-1}, R = 0.0345, R_w = 0.0500.
(9) Structural parameters for (4-methylpyridinium)$_2$Cu$_3$Br$_8$: monoclinic, space group $C2/c$, a = 28.207 (5) Å, b = 12.799 (2) Å, c = 14.735 (2) Å, β = 116.71 (1)°, Z = 8, ρ = 2.85 g/cm^3, μ = 160.3 cm^{-1}, R = 0.0561, R_w = 0.0500.
(10) Structural parameters for Cu$_2$Cl$_4$(4,4′-dimethyl-2,2′-bipyridine): monoclinic, space group $C2/c$, a = 17.063 (2) Å, b = 12.643 (2) Å, c = 7.278 (1) Å, β = 111.07 (1)°, ρ = 2.05 g/cm^3, Z = 4, μ = 36.2 cm^{-1}, R = 0.0331, R_w = 0.0364.
(11) Structural parameters for Cu$_2$Br$_4$(4,4′-dimethyl-2,2′-bipyridine): monoclinic, space group $C2/c$, a = 17.309 (6) Å, b = 13.267 (4) Å, c = 7.411 (2) Å, β = 110.69 (2)°, ρ = 2.64 g/cm^3, Z = 4, μ = 126.19 cm^{-1}, R = 0.0393, R_w = 0.0382.
(12) Bond, M. R.; Willett, R. D.; Rubins, R. S.; Zhou, P.; Zaspel, C. E.; Hutton, S. L.; Drumheller, J. E. *Phys. Rev. B*, submitted for publication.
(13) Pon, G.; Willett, R. D. To be submitted for publication.
(14) Plumer, M. L.; Hood, K.; Caille, J. *J. Phys. C: Solid State Phys.* **1988**, *21*, 4189.
(15) Bruinsma, R.; Zangwill, A. *Phys. Rev. Lett.* **1985**, *55*, 214.
(16) Rameseshа, S.; Rao, C. N. R. *Philos. Mag.* **1977**, *36*, 827.
(17) Gibbs, D.; Moncton, D. E.; D'Amico, K. L.; Bohr, J.; Grier, B. H. *Phys. Rev. Lett.* **1985**, *55*, 234.
(18) Bak, P.; von Boehm, J. *Phys. Rev. Lett.* **1978**, *42*, 122; *Phys. Rev. B* **1980**, *21*, 5297. Liebermann, R. *Statistical Mechanics of Periodic Frustrated Ising System*; Lecture Notes in Physics 251, Springer: Berlin, 1986.
(19) Bak, P.; Bruinsma, R. *Phys. Rev. Lett.* **1982**, *49*, 249; *Phys. Rev. B* **1983**, *27*, 5824.
(20) Fisher, M. E.; Selke, W. *Philos. Trans. R. Soc. London* **1981**, *31*, 1.

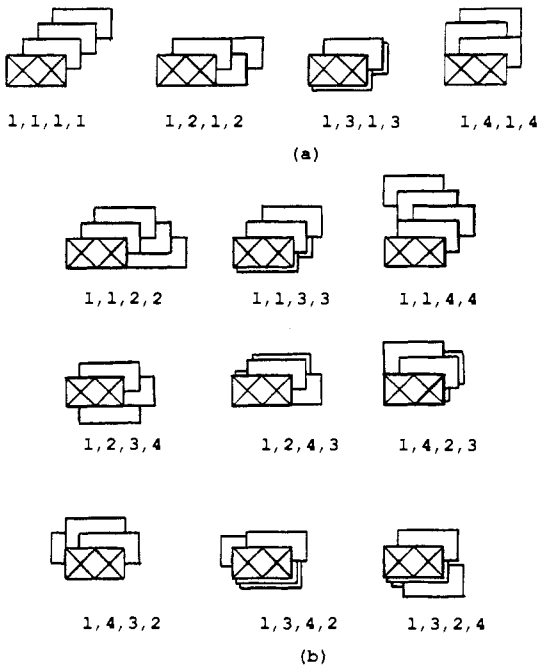

Figure 4. (a) Stable phases for nearest-neighbor stacking patterns. (b) Predicted stable competitive or next-nearest-neighbor phases.

the spins are restricted to lie in a plane, while the cubic anisotropy term further restricts the spin orientations toward the corners of a square in that plane. The following correspondences can be made

$$\vec{S} = (1, 0) \leftrightarrow \vec{t}_1$$
$$\vec{S} = (0, 1) \leftrightarrow \vec{t}_2$$
$$\vec{S} = (-1, 0) \leftrightarrow \vec{t}_3$$
$$\vec{S} = (0, -1) \leftrightarrow \vec{t}_4$$

where the components of the spin vectors refer to the coordinate system in Figure 3. The Hamiltonian for the isolated one-dimensional stacks is taken to be of the form

$$\mathcal{H} = K\sum_i \vec{S}_i\cdot\vec{S}_{i+1} + J\sum_i(\vec{S}_i\cdot\vec{S}_{i+1})^2 + D\sum_i(S_{i,x}S_{i+1,y} + S_{i,y}S_{i+1,x}) + K_2\sum_i \vec{S}_i\cdot\vec{S}_{i+2}$$

The three nearest-neighbor terms (K, J, D) describe the energy relations between consecutive pairs of translations. With K_2 small, four possible stable phases are predicted (at $T = 0$, since long-range order cannot exist at finite temperature for a 1d system), which are shown in Figure 4a. For convenience, the patterns are labeled by the subscripts of the sequence of $\vec{t}_k$ translation vectors defining the stacking arrangements. The ferrodistortive 1,1,1,1 and antiferrodistortive 1,3,1,3 phases are stable for $K \ll 0$ and $K \gg 0$, respectively, while the vertical 1,4,1,4 and horizontal 1,2,1,2 propagation patterns are found when $D \gg 0$ and $D \ll 0$, respectively. All four of these polytypes are now observed experimentally with the report of the $Cu_2X_4L^2$ structures.

The inclusion of the next-nearest-neighbor interaction leads to a very rich series of nine competition phases (analogous to the ↑↑↓↓ phase of the next-nearest-neighbor spin $^1/_2$ Ising model), as shown in Figure 4b. The lower two rows contain three sets of degenerate entantiomorphic pairs of stacking patterns. The 1,1,2,2 pattern reported in this paper is the first of these competition phases to be observed experimentally.

The $T = 0$ phase diagram for this Hamiltonian is extremely rich, with regions of stability predicted for the four nearest-neighbor phases as well as for all nine competition patterns. This is illustrated in Figure 5 for a D, K section through the four-parameter space with $K_2 < 0$ and $J = 0.5\,K_2$. This particular section includes all four nearest-neighbor phases, as well as five regions where competition phases are predicted to be stable. The

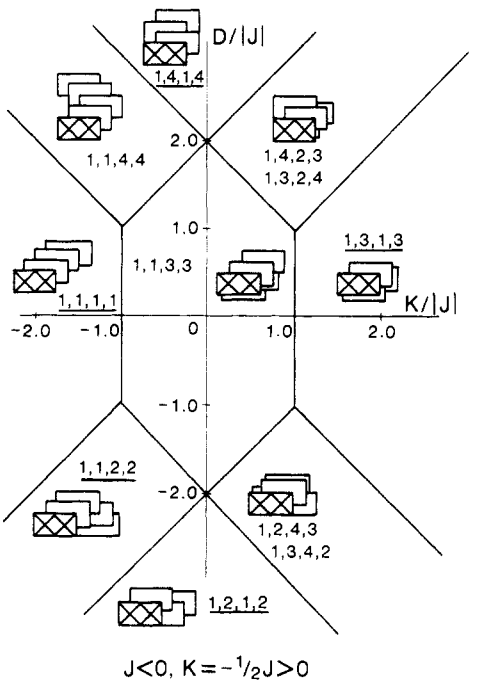

Figure 5. Section of the predicted phase diagram in the D, K plane for $K_2 < 0$ and $J/|K| = 0.5$. Underlined phases have been observed experimentally. Only one envelope diagram has been included for the two regions containing degenerate enantiomorphic pairs.

distribution of known phases (underlined in Figure 5) is such the currently unobserved phases lie in regions of parameter space intermediate between the areas occupied by the known phases. Thus, just as with the 1,1,2,2 phase, realization of other competition phases can be anticipated as design strategies are developed based upon interpretation of the factors that determine the values of the various energy parameters.

Acknowledgment. The support of NSF Grant DMR-8803382 is gratefully acknowledged.

Registry No. (4-methylpyridinium)$_2Cu_3Cl_8$, 116155-35-2; (4-methylpyridinium)$_2Cu_3Br_8$, 129029-38-5; Cu_2Cl_4(4,4'-dimethyl-2,2'-bipyridine), 128900-79-8; Cu_2Br_4(4,4'-dimethyl-2,2'-bipyridine), 128900-80-1.

Contribution from the Department of Chemistry, Princeton University, Princeton, New Jersey 08544

A Simple Synthesis of 3-Bromo-*o*-carborane[1]

Ji Li and Maitland Jones, Jr.*

Received March 7, 1990

Although more than one synthesis of 3-bromo-*o*-carborane (**1**) appears in the literature, no current route makes this potentially useful compound easily available. We report here a simple modification of one synthesis of **1** that provides this molecule in good yield and high purity.

One multistep source of **1** is the Sandmeyer reaction of 3-amino-*o*-carborane (**2**), itself available in nearly quantitative yield from $(B_{10}C_2H_{12})^{2-}$.[2,3] The yield of **1** from this procedure seems not to be reported, but that of the related 3-chloro-*o*-carborane is 47.5%.

(1) Support for this work by the National Science Foundation through Grant CHE 8800448 is gratefully acknowledged.
(2) Zakharkin, L. I.; Kalinin, V. N.; Gedymin, V. V. *J. Organomet. Chem.* **1969**, *16*, 371.
(3) Zakharkin, L. I.; Kalinin, V. N. *Izv. Akad. Nauk SSSR, Ser. Khim.* **1968**, 671.

